In-silico simulation of obstetric forceps placement using the Hilber-Hughes-Taylor implicit integration method with contact constraints

Rudy Lapeer and Omar Valladolid García

University of East Anglia, Norwich NR4 7TJ, UK,
r.lapeer@uea.ac.uk

Abstract. Obstetric forceps are used as an instrumental delivery method when physiological childbirth fails to progress. The technique comprises the insertion of two stainless steel blades in the vagina that are subsequently coupled to make firm contact with the fetal head. In this paper, we assessed the effect of symmetric against asymmetric placement of the blades around the fetal head. Assessment was facilitated in-silico by creating mesh models of the fetal head and forceps and conducting implicit dynamic finite element analyses using the Hilber-Hughes-Taylor integration method, with imposed contact constraints between the virtual head and forceps. We observed that asymmetric forceps blade placement causes increased local deformations and strains that may potentially be harmful to the fetus. We conclude that forceps traction should not be applied when blades are asymmetrically placed around the fetal head.

Keywords: Finite Element Analysis (FEA), Finite Element Method (FEM), Assisted Vaginal Delivery (AVD)

1 Introduction

Obstetric forceps delivery is one of two main assisted vaginal delivery (AVD) interventions when physiological (natural) delivery fails to expel the fetus. The other intervention is vacuum extraction (VE) that uses a suction cup that is secured on the fetal scalp via a vacuum and is connected to a chain (or nowadays a plastic cable) held by the operator to exert traction. The latter is a limitation of VE as it does not allow to rotate the fetal head during extraction thus reducing manoeuvrability.
Obstetric forceps consist of a pair of blades, i.e. a left and right blade, that are inserted one by one in the womb, around the fetal scalp, and then assembled via a slot-locking mechanism - see Figure 1(Top). The extent of the contact areas of the blades with the fetal scalp depend on how well the blades have been placed. The application of traction is a fairly slow process with minimal acceleration at the start and can therefore be considered as quasi-static. Obstetric forceps delivery is often perceived as potentially dangerous yet it is a safe procedure

provided that the blades are placed symmetrically around the fetal scalp [1]. In this study we aim to simulate the effect of the forceps on the fetal scalp when it is placed correctly (symmetric) and incorrectly (asymmetric).

Fig. 1. Top: Disassembled clinically approved Neville Barnes forceps, showing the slot-locking mechanism. Bottom: Lateral view of forceps assembled around a replica fetal head model (ESP ZKK-422-P).

2 Background

2.1 Obstetric forceps simulation

In previous research [2], we approximated the forceps-to-head interaction, that is a quasi-static mechanical contact process, via a static implicit FEA by identifying the contact areas between forceps blades and fetal scalp. Realistic normal forces (representing contact) and tangential forces (representing traction) obtained from the literature [3] were then applied to those elements on the fetal scalp identified as being in contact with the forceps. As such, the forceps itself was not part of the FEA so there was no need of imposing contact constraints.

Although results appeared to be clinically meaningful, the omission of the forceps in the FEA reduced experimental flexibility to assess different positions of the blades around the scalp. Moreover, its potential of using the simulation for hands-on training when for example coupled to a suitable haptics device [4, 5] was limited.

In recent preliminary experiments we included the forceps as a FE model in the FEA [6]. In the current paper, we will present further improvements via two series of numerical experiments (simulations) that include the modelling of a fluid cavity to represent the fetal brain and the comparison of implicit FE methods.

2.2 Volume conservation

Fetal head moulding (FHM) is the deformation of the fetal scalp caused by the contact of the head with the maternal anatomical structures during the first and second stages of labour [7]. Forceps application, in particular when blades are placed asymmetrically, will significantly worsen FHM [2]. Neither of the previous two studies [2, 7] considered the potential effect of the fetal brain on FHM due to it being near incompressible (Poisson's rate $\eta \approx 0.5$). Since we are not studying the effect of FHM on the fetal brain, a complex FE model of the brain is not needed but instead, we can install a fluid cavity inside the fetal head that will conserve volume under deformation. This implies that the original volume V_0 and the deformed volume V_d need to be the same. Putting this in equation form gives:

$$\Delta V = V_d - V_0 = 0 \tag{1}$$

2.3 Implicit Dynamic FEA

The quasi-static nature of the closure of, and traction on, the forceps blades implies that global accelerations are small and potentially negligible (see section 3.3). In such cases implicit dynamic FEA is considered to be more suitable than explicit FEA. In fact, the terms implicit and explicit in FEA relate to the integration methods that function as solvers of the FE equations. Explicit integration methods such as the central difference method do not require stiffness matrix factorisation and tend to be faster than implicit methods. However, since simulation speed was not a criterion in this study we consider implicit methods instead.

As mentioned before, due to the quasi-static nature of the problem, we can consider three implicit solvers, i.e. static, quasi-static and dynamic. Since we adopt non-linear geometry settings as part of our FEAs we can use a static analyis as a proxy for a quasi-static problem since the loads are incremented in virtual time steps. We will use the ABAQUS SIMULIA (AS) software to run the experiments. For dynamic implicit analyses, AS distinguishes between quasi-static and dynamic settings.

The dynamic FE equation to be solved is [8] :

$$M\ddot{U}_t + C\dot{U}_t + KU_t = R_t \tag{2}$$

Where U, $\dot{U}$ and $\ddot{U}$ are respectively, the nodal displacement, velocity and acceleration vectors; M,C and K are respectively, the mass, damping and stiffness matrices; R is the vector of externally applied loads; and t is the current time.

Quasi-static procedures in AS use the backward (implicit) Euler integration method [9], with time increment (step) Δt:

$$\begin{aligned} U_{t+\Delta t} &= U_t + \Delta t \dot{U}_{t+\Delta t} \\ \dot{U}_{t+\Delta t} &= \dot{U}_t + \Delta t \ddot{U}_{t+\Delta t} \end{aligned} \tag{3}$$

Implicit dynamics procedures in AS use the Hilber-Hughes-Taylor (HHT) integration method [10]:

$$\begin{aligned} U_{t+\Delta t} &= U_t + \Delta t \dot{U}_t + \Delta t^2((\tfrac{1}{2} - \beta)\ddot{U}_t + \beta \ddot{U}_{t+\Delta t}) \\ \dot{U}_{t+\Delta t} &= \dot{U}_t + \Delta t((1-\gamma)\ddot{U}_t + \gamma \ddot{U}_{t+\Delta t}) \\ \beta &= \tfrac{1}{4}(1-\alpha)^2, \gamma = \tfrac{1}{2} - \alpha, -\tfrac{1}{3} \leq \alpha \leq 0 \end{aligned} \tag{4}$$

3 Study design

Two sets of FE experiments (simulations) will be run. An **initial experiment** with basic geometric models to test out parameters that include the traction velocity and the mesh complexity of the fetal head, and select the optimal parameter settings based on the accuracy of the results and the stability of the analysis. These are then fed into the **main experiment** that has more realistic, but also distinctly more complex, geometric models.

3.1 Material properties

The fetal cranium consists of fetal cranial bone that exhibits orthotropic material behaviour [11]. The soft tissue areas, known as fontanelles and sutures, exhibit the same material characteristics as fetal dura mater [12]. The skull base is considered to be cortical bone [7]. The forceps blades are in stainless steel [6]. Table 1 has the relevant material properties needed in the FEA and also includes the types of elements used.

3.2 Models

There are two sets of **geometric FE models** for each of the two experiments:

- **Initial Experiment:** A simple sphere, with two areas identified as the anterior and posterior fontanelles, functions as a basic fetal cranium. Four different meshes with complexities of respectively 768, 3072, 12288 and 20480 triangular shell elements were used. They are shown in the top row of Figure 4. The obstetric forceps are hemi-cylindrical shells with the curvature derived from a real forceps and are shown at the top of Figure 2.
- **Main Experiment:** A detailed FE model of the fetal cranium with 18742 elements is shown at the bottom of Figure 2. It is based on a laser scan of the replica fetal head model (ESP ZKK-422-P) as shown in Figure 1. The obstetric forceps FE model is shown in the middle of Figure 2.

Both geometric head models have a fluid cavity inside as a proxy for the incompressible brain.

3.3 Loads, contact and boundary conditions

In an earlier simulation experiment, not reported here, we applied forces to the FE forceps model for both closure and traction based on values provided in the literature [3]. This approach caused various instability issues. Firstly, once the forceps was closed and the left and right forceps handles were in contact, it was difficult to keep them in stable contact during the traction stage. Secondly, it was difficult to estimate the net traction force without ending up with unrealistically high traction velocities. Considering obstetric forceps traction is fairly slow at the start of the intervention (quasi-static) we abandoned the use of traction forces and applied a constant traction velocity instead.
Based on the observation of real forceps applications, traction velocities range between 1mm to 12mm/s. These velocities were applied in the positive z-direction. For the initial experiment, blades were pulled over a distance of 25mm to maximise the bulging of the anterior fontanelle without slipping off the sphere.
For the main experiment a more realistic displacement, typically observed at the onset of forceps traction (pull), of 2.5mm was applied.
The ABAQUS SIMULIA (AS) software has different modes for contact interactions. Due to the complexity of the models in contact and the possibility of multiple, separate contact areas between the two forceps blades at each side of the fetal head, we adopted the finite sliding, surface-to-surface, general contact option that uses the Augmented Lagrange contact model [13].
To conserve the fetal cranium's volume (Section 2.2) we added a fluid cavitiy interaction. This is facilitated in AS by defining a cavity point in the centre of the cranium (e.g. the centre of gravity) and then define the cavity surface surrounding the cavity point, which in our case is the inner surface of the cranial vault. Fluid interactivity properties were set to those of water, i.e. density, $\rho = 1,000$ kg/m^3 and bulk modulus, $K = 2.5$ GPa.
Finally, both head and forceps needed to be constrained to avoid unrealistic rigid body motion. Figure 3 shows the boundary conditions for both initial and main experimental setups.

4 Results

4.1 Initial experiment

Due to using simple spherical models with smooth curvature, the initial experiment was designed to test out the effect of mesh complexity and traction speed. It started by closing the forceps to bring them in contact with the fetal head. This has to happen fairly slowly to avoid abrupt contact so a velocity of 1mm/s for 3s was applied. The result of this can be seen in Row 2 of Figure 4 where a slight indentation on both left and right sides of the sphere becomes visible due

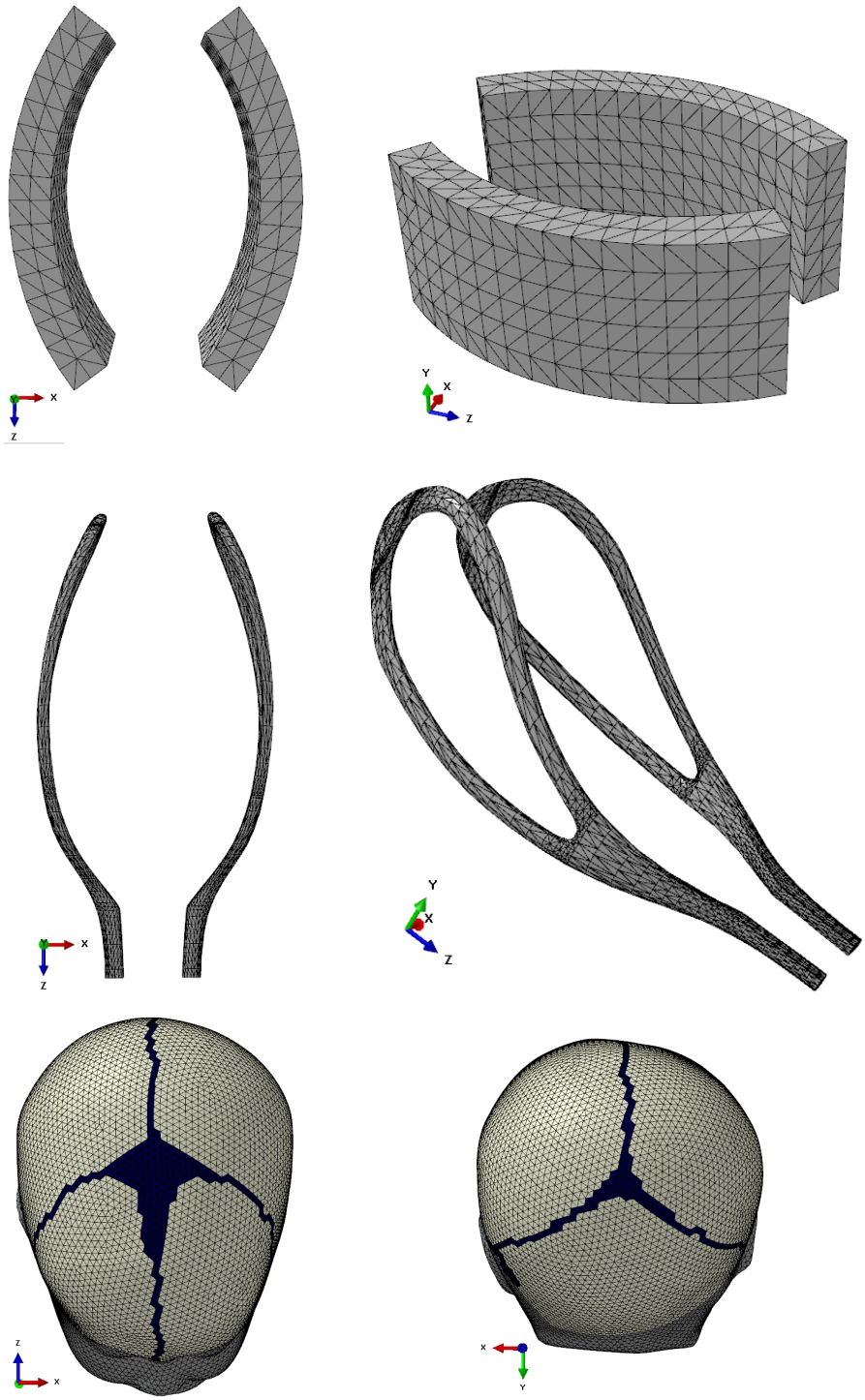

Fig. 2. Top: Basic forceps model front and side view. Middle: Realistic Neville-Barnes forceps model front and side view. Bottom: Detailed FE mesh model of the fetal cranium with 18,742 elements. Left shows the top view with the anterior fontanelle and sutures (dark blue) and right shows the smaller posterior fontanelle. Fetal cranial bones are in light gray and the skull base and facial bones in dark gray.

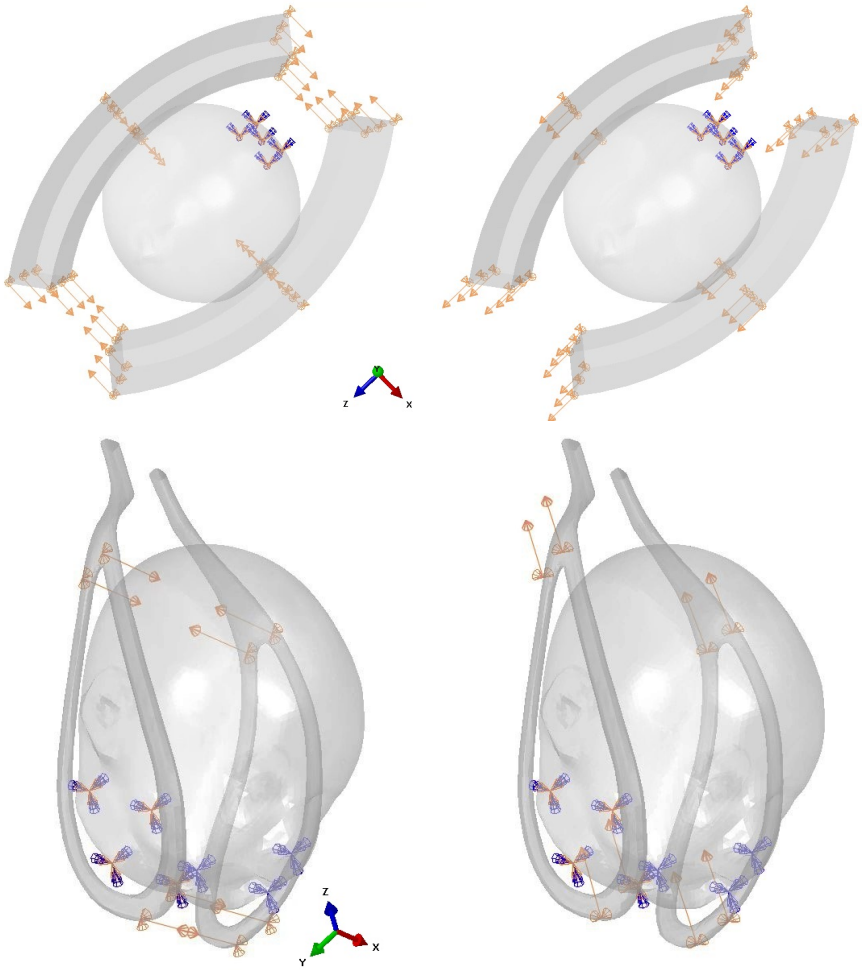

Fig. 3. Boundary conditions. Top from left to right: Initial experiment, closure then traction. Bottom from left to right: Main experiment, closure then traction. Both fetal head models are encastred at the neck and the complex model (bottom) also at the front of the face to avoid rigid body rotation around the Y-axis.

Property	Scalp bones	Fontanelles/sutures	Skull base	Forceps
Thickness (mm)	0.75	0.75	2	N/A
Mass density (kg/m^3)	1,000	1,000	1,200	7,800
Material type	Orthotropic Linear elastic	Isotropic Hyperelastic	Isotropic Linear elastic	Isotropic Linear elastic
E1 (GPa)	3.86	-	4.46	209
E2 (GPa)	0.965	-	-	-
G (GPa)	1.582	-	-	-
μ_{12}	0.22	-	0.21	0.30
μ_{21}	0.055	-	-	-
C1 (MPa)	-	1.18	-	-
C2 (MPa)	-	0.295	-	-
Element type	S3	S3	C3D4	C3D4

Table 1. Material properties of the three main components of the fetal skull, i.e. the fetal cranial bones [11], the skull base [7], the fontanelles and sutures [12], and steel for the obstetric forceps models [6]. The bottom row gives the finite element types as used in the AS software where S3 is a triangular shell element and C3D4 is a solid tetrahedral element.

to the contact with the left and right blades. Next we applied traction forces in the Z-direction at different velocities ranging from 1mm/s to 12.5mm/s over a distance of 25mm. The end result as shown in the fourth row of Figure 4 is for a velocity of 5mm/s (5s duration). Note that the final shape after deformation was independent of the traction velocity but processing times did vary. At each stage, the inside volume of the head was calculated and ΔV was consistently less than 0.009%[1]. There is also a clear difference between the shape after deformation between different mesh complexities where the most complex mesh exhibits deeper indentations on both sides where there is contact with the forceps blades and a clearly bulging anterior and posterior fontanelle (Column 4, Row 4 in Figure 4), as compared to coarser meshes (Columns 1-3). Therefore a mesh complexity of the same order of magnitude was adopted for the complex head model in the main experiment. We also tried out the three different implicit integration methods, i.e. static, quasi-static (backward Euler) and dynamic (HHT).
Neither static nor quasi-static analyses managed to converge to the full traction distance (25mm). Larger initial time steps failed to converge and in the long run had to be reduced below an acceptable minimal time step value[2]. The likely explanation is that both static and quasi-static methods use too basic displacement

[1] Although not shown here, we ran the same experiments without a fluid cavity. Shapes after deformation also showed the lateral indentations but the bulging of the fontanelles was substantially less and the volume decreased significantly with a ΔV greater than 4.0% thus confirming the importance of volume conservation for added realism.

[2] The maximum time step was 10% of the total analysis duration and varied between 0.2s to 2.5s. The absolute minimal time step was set to 1E-06s.

updates to guarantee convergence for the complex multi-contact problem that was attempted in this experiment. Unlike the HHT integration method, that uses a higher-order displacement update scheme (see Equation 4) and therefore converged quicker for all initial experiments and was therefore adopted for use in the main experiment.

4.2 Main experiment

Based on results derived from the previous experiment, here we ran two analyses on the complex and more realistic models of forceps and fetal head. We compared two positions of the forceps relative to the fetal head: **symmetric** at 0 degree angle of the forceps with the Z-axis, and **asymmetric** at +10 degrees of forceps rotation (CCW) around the Z-axis, simulating an incomplete internal rotation. Closure was performed at 1mm/s for 3s, as in the initial experiment. Traction was sustained for 0.5s at 5mm/s over a distance of 2.5mm.
Figure 5 shows the results for **symmetric** placement. At the top (Row 1) is the undeformed head in three directions. Row 2 shows the displacement U (in m) after closure. The next three rows show displacement U at the start, the midde and the end of a traction cycle. Although the displacement is high, there is very little deformation of the fetal head as, due to being in good contact with the blades, all of it is rigid body displacement in the direction of traction (Z-axis).
Figure 6 shows the result for **asymmetric** placement. Despite looking less "colourful" than the symmetric plots, most of the overall displacement is deformation and the forceps blades are slipping due to poor contact. In particular, the deformation in the facial areas is high where the left blade is pressing hard on the jaw bone. This is particularly visible in the lateral view at full traction (Column 1, Row 5 of Figure 6). Note that deformations in both Figures 5 and 6 have been scaled by a factor 2.0 to make the head shape changes clearer.
Figure 7 shows the combined (min,max) principal strain for symmetric and asymmetric placements. The strain where the tip of the forceps is in contact with the (left) jaw is maximum compressive at around -0.3 for asymmetric placement and is only around -0.03 for symmetric placement, further illustrating the high local deformations for asymmetric placement.

5 Conclusion

We have presented a series of FE experiments to model the application of obstetric forceps to the fetal head during childbirth. In comparison with previous work [2][6], we built a more robust FEA framework to obtain more realistic solutions for a complex biomechanical contact problem. This framework was first tested on simplified geometric representations of the fetal head and forceps as part of the initial experiment that included a fluid cavity to model the incompressible fetal brain; the comparison of different implicit FE methods (static, quasi-static and dynamic); the comparison of different mesh complexities; and the comparison of different forceps traction velocities modelled as boundary conditions.

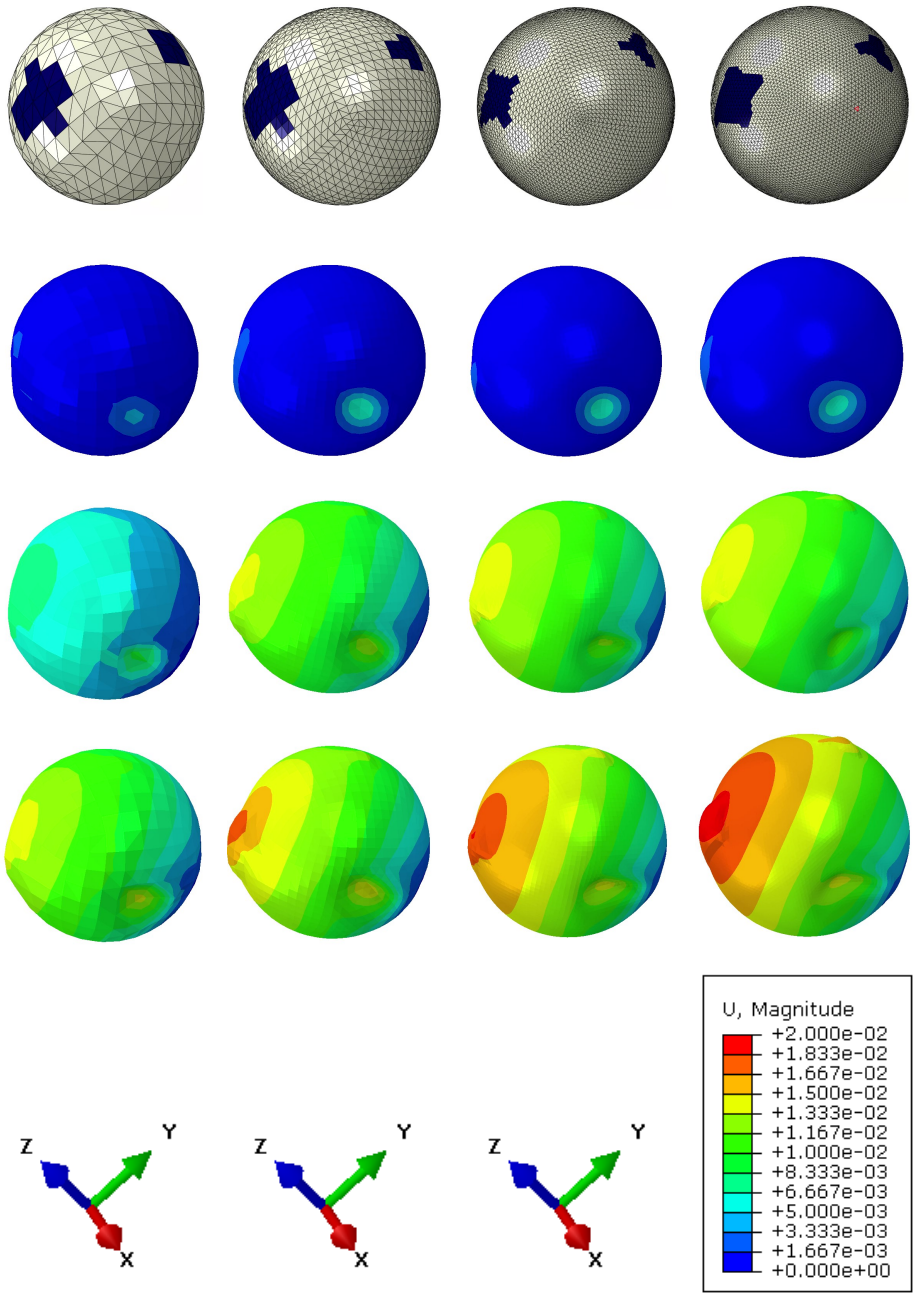

Fig. 4. Initial experimental results. Each column shows an increasingly more complex mesh with 768, 3072, 12288 and 20480 elements respectively. Row 1: Undeformed mesh before forceps application. Row 2: Displacement U, in all directions, in m, after closure. Row 3: Displacement U in m, halfway during traction. Row 4: Displacement U in m, at the end of the traction cycle of 5s. Traction speed was 5mm/s.

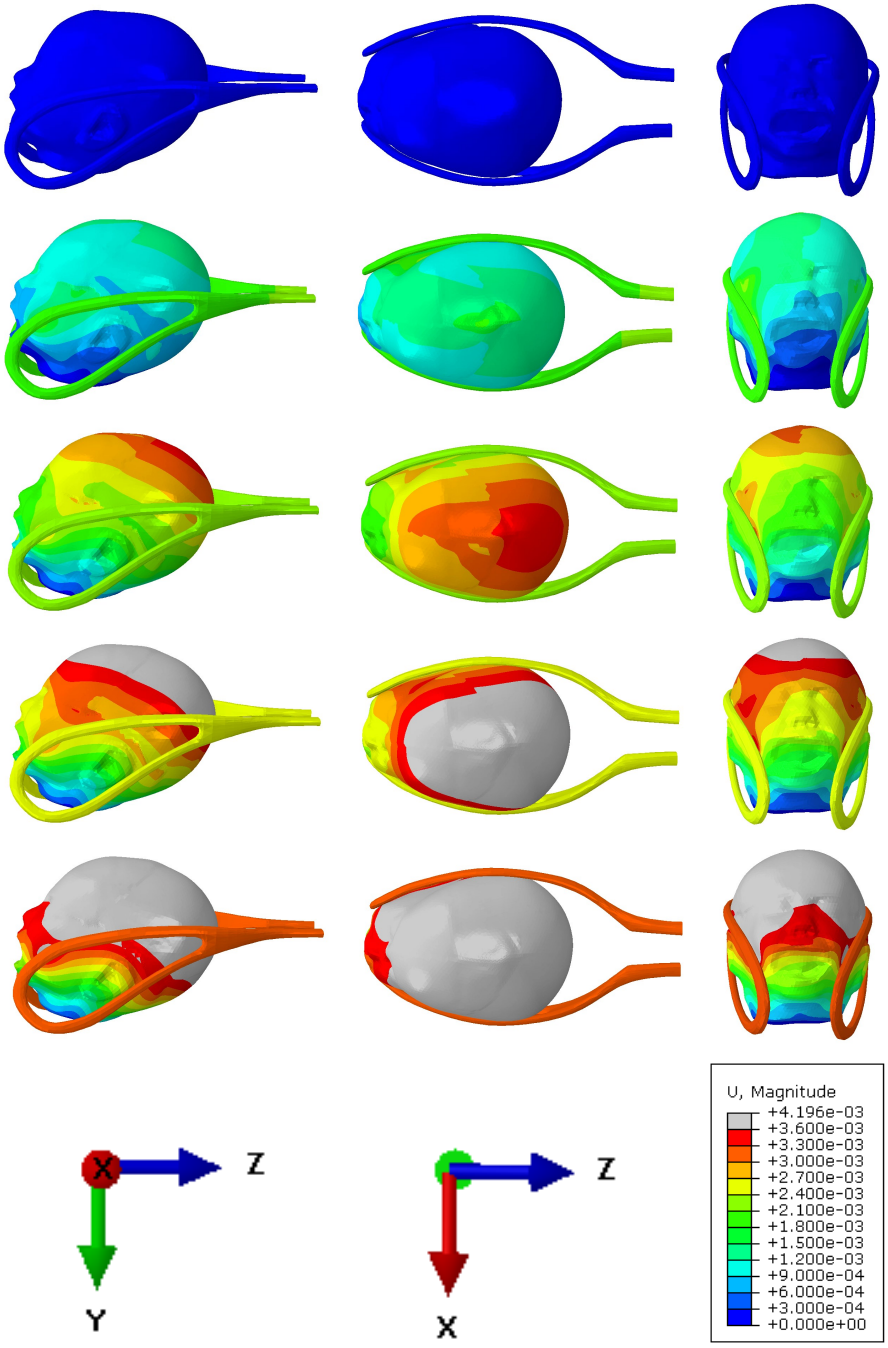

Fig. 5. Displacement in m for symmetric forceps placement. From top to bottom: Open, Close, Pull 1mm, Pull 1.5mm, Pull 2.5mm. From left to right: Lateral, Top and Front views. Deformation scale factor is 2.0. See text for discussion.

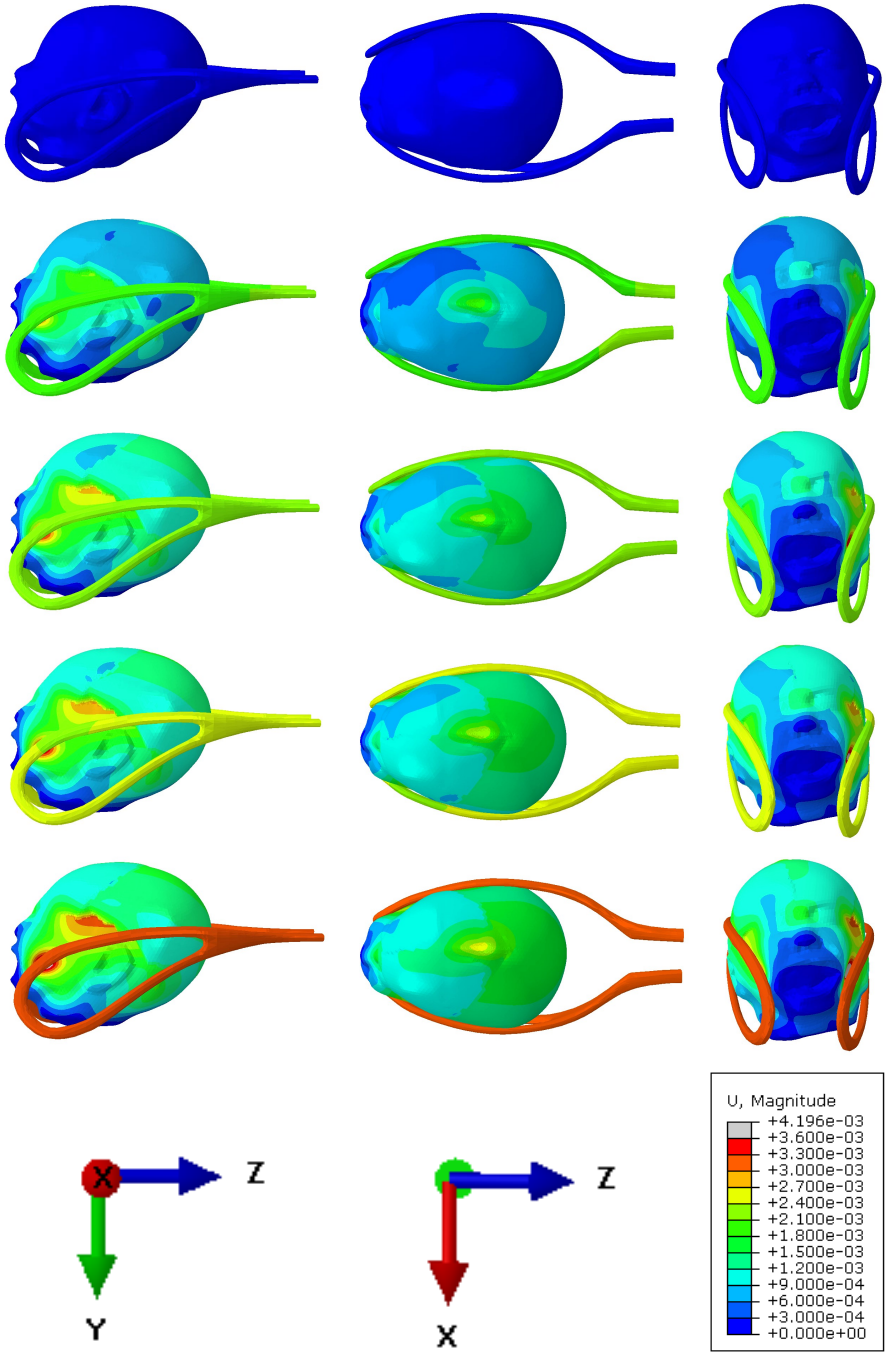

Fig. 6. Displacement in m for asymmetric forceps placement (head internal rotation short of 10 degrees). From top to bottom: Open, Close, Pull 1mm, Pull 1.5mm, Pull 2.5mm. From left to right: Lateral, Top and Front views. Deformation scale factor is 2.0. See text for discussion.

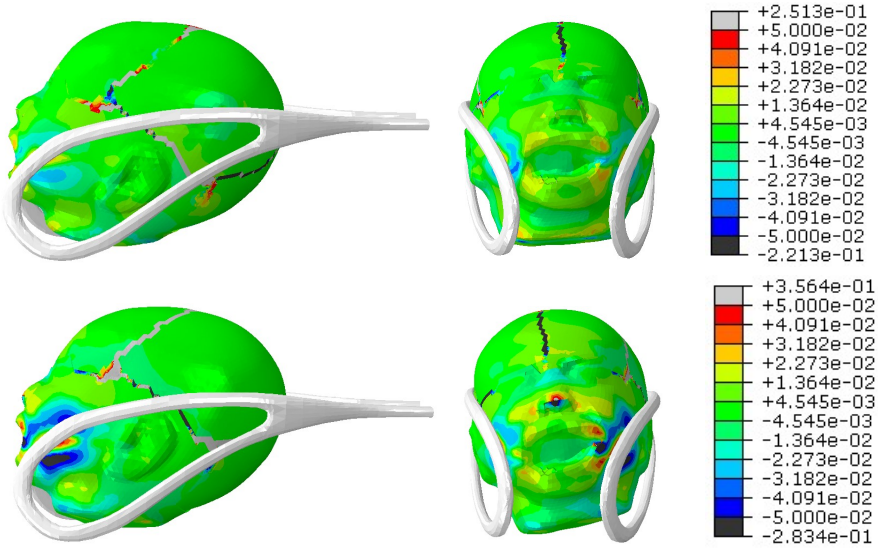

Fig. 7. Combined (min,max) in-plane principal strains for symmetric (top) and asymmetric (bottom) forceps placements respectively.

Based on the successful validation of basic models in the initial experiment, we derived optimal parameter settings that were then applied to the more complex and realistic geometric models of the fetal head and forceps, as part of the main experiment. Two analyses were run with symmetric and asymmetric forceps placement respectively. It was shown that asymmetric placement causes large local deformations that could potentially cause facial injuries and potentially damage the fetal cranial bones and the underlying fetal brain. This result is in agreement with observations from O'Mahony et al. [14] who report comparisons between the use of obstetric forceps and vacuum extraction and observed that facial injury is more likely to happen for forceps delivery due to its surrounding contact with the fetal head, and exacerbated by asymmetric placement.

Considering the quasi-static nature of the obstetric forceps application, the use of a Dynamic Implicit (DI) solver such as HHT is preferred over a Dynamic Explicit solver that is more suitable to problems that include high velocities and/or impact. However, the disadvantage of a DI solver is that the runtime for complex problems is very high so explicit analysis will be looked at in future work.

In [2] we adopted a simpler, non-contact, approach to model forceps interaction as compared to the contact-based approach in this paper. Though we did test this simpler approach on heads that already exhibited fetal head moulding (pre-moulded) as caused by the phsyiological (normal) birth process. This was omitted here to avoid added runtime complexity but will be investigated in future experiments, together with varying the material properties of the fetal cranium and fontanelles, to evaluate their effect.

Finally, real-time performance of a contact-based forceps simulation could be achieved using the BirthView "digital twin" simulator [13]. BirthView uses the Total Lagrangian Explicit Dynamics (TLED) method [15] on the GPU and is capable of simulating a physiological childbirth in real-time.

References

1. Dupuis, O., Decullier, E., Clerc, J., Moreau, R., Pham, M.T., Bin-Dorel, S., Brun, X., Berland, M., Redarce, T.: Does forceps training on a birth simulator allow obstetricians to improve forceps blade placement? European Journal of Obstetrics & Gynecology and Reproductive Biology 159(2), 305–309 (2011)
2. Lapeer, R., Audinis, V., Gerikhanov, Z., Dupuis, O.: A computer-based simulation of obstetric forceps placement. In: International Conference on Medical Image Computing and Computer-Assisted Intervention. pp. 57–64. Springer (2014)
3. Chachava, K., Vashakidze, P., Kacharava, R., Sarkisian, S., Chkhatarashvili, N.: Measurement of forces during application of obstetric forceps. Biomedical Engineering 3(2), 83–85 (1969)
4. Moreau, R., Pham, M.T., Brun, X., Redarce, T., Dupuis, O.: Assessment of forceps use in obstetrics during a simulated childbirth. The International Journal of Medical Robotics and Computer Assisted Surgery 4(4), 373–380 (2008)
5. Lapeer, R., Chen, M., Villagrana, J.: Simulating obstetric forceps delivery in an augmented environment. Augmented environments for Medical Imaging including Augmented Reality in Computer-aided Surgery (AMI ARCS'04) (2004)
6. García, O.V., Lapeer, R.: Contact-constrained finite element analysis to evaluate obstetric forceps placement. In: 2024 E-Health and Bioengineering Conference (EHB). pp. 1–4. IEEE (2024)
7. Lapeer, R., Prager, R.: Fetal head moulding: finite element analysis of a fetal skull subjected to uterine pressures during the first stage of labour. Journal of biomechanics 34(9), 1125–1133 (2001)
8. Bathe, K.J.: Finite element procedures. Klaus-Jurgen Bathe (2006)
9. Epperson, J.F.: An introduction to numerical methods and analysis. John Wiley & Sons (2013)
10. Hilber, H.M., Hughes, T.J., Taylor, R.L.: Improved numerical dissipation for time integration algorithms in structural dynamics. Earthquake Engineering & Structural Dynamics 5(3), 283–292 (1977)
11. McPherson, G.K., Kriewall, T.J.: The elastic modulus of fetal cranial bone: a first step towards an understanding of the biomechanics of fetal head molding. Journal of biomechanics 13(1), 9–16 (1980)
12. Bylski, D.I., Kriewall, T.J., Akkas, N., Melvin, J.W.: Mechanical behavior of fetal dura mater under large deformation biaxial tension. Journal of biomechanics 19(1), 19–26 (1986)
13. Lapeer, R., Gerikhanov, Z., Sadulaev, S.M., Audinis, V., Rowland, R., Crozier, K., Morris, E.: A computer-based simulation of childbirth using the partial dirichlet–neumann contact method with total lagrangian explicit dynamics on the gpu. Biomechanics and modeling in mechanobiology 18(3), 681–700 (2019)
14. O'Mahony, F., Hofmeyr, G.J., Menon, V.: Choice of instruments for assisted vaginal delivery. Cochrane Database of Systematic Reviews (11) (2010)
15. Miller, K., Joldes, G., Lance, D., Wittek, A.: Total lagrangian explicit dynamics finite element algorithm for computing soft tissue deformation. Communications in numerical methods in engineering 23(2), 121–134 (2007)